JOURNAL OF MATERIALS SCIENCE 21 (1986) 3863–3872

Crystallization of Zr–Ni metallic glasses

C. G. MCKAMEY, D. M. KROEGER, D. S. EASTON, J. O. SCARBROUGH
Metals and Ceramics Division, Oak Ridge National Laboratory, Oak Ridge, Tennessee 37831, USA

The crystallization of Zr–Ni metallic glasses of composition between 55 and 70 at % Zr has been investigated using differential scanning calorimetry (DSC) and X-ray diffraction (XRD). The samples were prepared by splat quenching in an arc-hammer device. Transformation temperatures, effective activation energies, and enthalpy changes are reported as a function of composition. Results of XRD patterns obtained as a function of annealing temperature in the DSC are presented. A high temperature exothermic DSC peak and XRD patterns indicate the presence of a metastable phase which occurs between 57 and 63.5 at % Zr. The results tend to support suggestions of a connection between the short range structure of the glass and the crystalline phase to which it transforms. It was found that the metastable phase, whose presence is strongest at 57 to 59 at % Zr, and the process of phase separation around the eutectic composition (63.5 at % Zr) play important roles in the crystallization process.

1. Introduction

Metallic glasses are metastable, and given the proper combination of temperature and time, will crystallize either directly to expected equilibrium phases or through complex stages involving intermediate crystalline phases. Potentially useful mechanical, magnetic and electrical properties may be lost during the transformations preceding and during crystallization. An understanding of these transformations is essential, not only for the design of metallic glasses with more stable properties, but also to the understanding of the relationship between the glass structure and the crystalline phases to which the glass transforms.

In this paper we report on the crystallization behaviour of the Zr–Ni metallic glass system between 55 and 70 at % Zr. This study was motivated by results of a previous study of the compositional dependence of parameters derived from the low-temperature specific heat [1, 2]. In that study evidence was found for the presence of two types of short-range order in the amorphous state, indicating that phase separation occurs in this composition range in the Zr–Ni system. Several other researchers have studied crystallization in this system in recent years and have reported data from thermal analysis which were in some cases conflicting [3–13]. All these researchers conducted their studies on melt-spun ribbons which are prone to contamination from the spinning atmosphere or from the crucible material during melting [14]. For that reason we chose to prepare samples for this study by splat-quenching. Differential scanning calorimetry (DSC) and X-ray diffraction (XRD) were used to characterize the crystallization sequence. A second part of this study involving transmission electron microscopy to characterize the crystal morphologies will be presented in a later paper.

2. Experimental procedures

Alloy buttons of Zr–Ni compositions between 55 and 70 at % Zr were prepared by arc-melting high purity zirconium and nickel in an argon atmosphere on a water-cooled copper hearth. The difference in the weights of the alloys measured before and after casting indicated that the compositions deviated from nominal values by no more than ± 0.2 at %. Splats of each alloy were produced in an argon atmosphere by using a piston and anvil splat-quenching device which produces cooling rates of approximately 10^6 K sec^{-1} [15]. The 20 to 30 μm thick foils produced were studied with a Philips Norelco diffractometer using Cu$K\alpha$ radiation and no splat was further studied which did not exhibit the broad diffuse pattern characteristic of an amorphous metal.

A DSC-2 differential scanning calorimeter (DSC) (Perkin–Elmer, Norwalk, Connecticut) was used for thermal analysis of the crystallization process. Samples weighing between 2 and 4 mg were placed in gold pans and heated under flowing argon at rates of 5, 10, 20, 40 and 80 K min^{-1} through the transformation peaks. After the different heating rates were corrected using the melting temperature of zinc (692.65 K), the onset of crystallization (T_x) and the temperature of each transformation peak (T_{p_1}, T_{p_2}, etc.) were recorded. The effective activation energy (ΔE) for each peak was determined using the Kissinger method [16, 17] in which ΔE is given by the slope of a plot of $\ln(\dot{T}/T_p^2)$ versus T_p^{-1}, where $\dot{T}$ is the heating rate and T_p is the temperature at the peak. The change in enthalpy during crystallization was determined from the area under the DSC trace. An average value, obtained by measuring the areas of four to five different pieces of the same splat, was used to calculate the enthalpy change (ΔH) for each alloy. At most compositions more than one splat-cooled sample was tested, producing more than one value for T_x, T_p, ΔE, and ΔH, although in some figures only average values are shown. Also, since some compositions exhibited more than one DSC peak and the process associated with

0022–2461/86 $03.00 + .12

each peak was not known, the peaks for each sample were numbered consecutively as a means of identification. Values were then designated as T_{p_1} and ΔE_1 for the first DSC peak, etc.

To correlate phase transformations with peaks in the DSC, several compositions were selected for XRD analysis. The specimens were sealed in gold pans and heated in the DSC at 80 K min^{-1} to the desired point on the DSC curve, then immediately cooled to room temperature at 320 K min^{-1}. X-ray diffraction patterns were then obtained on these specimens.

3. Results

3.1. Thermal analysis by DSC

The exothermic responses produced as the Zr–Ni splats were heated in the DSC through the crystallization transformations were found to vary with composition. Fig. 1 presents the peaks produced at a heating rate of 20 K min^{-1} as a function of temperature for the range of compositions studied. The DSC traces were normalized to a 3 mg weight sample, position represents the amount of heat given off when a 3 mg sample of that composition crystallizes at a constant heating rate. Several observations can be made regarding this figure.

1. Overall, the onset of the crystallization process decreases in temperature as zirconium content is increased.

2. Beginning at the $Zr_{57.1}Ni_{42.9}$ composition and continuing up to the eutectic composition at $Zr_{63.5}Ni_{36.5}$, the DSC pattern exhibits a small exotherm which is more than 100 K above the main transformation peak(s). The temperature at the peak varies with composition and is a maximum at 59 at % Zr. Likewise, the peak tends to increase and decrease in size following the same compositional dependence. As will be discussed below, this peak is associated with the transformation of a metastable phase (which forms during the lower temperature transformations) to the ZrNi and Zr_2Ni equilibrium phases [18, 19].

3. The DSC traces for compositions of 57 to 59 at % Zr show single sharp and symmetric crystallization peaks, suggesting that only one transformation process is occurring. Below this composition range, a leading shoulder gradually enlarges until the DSC peak is definitely asymmetric at 55 at % Zr. At 67 and 69 at % Zr the trace again shows only one sharp peak.

4. The DSC traces for compositions between 60 and 66.5 at % Zr are characterized by multiple peaks, indicating a complicated crystallization process involving several different steps. At 60 at % Zr a small second peak is seen during the low-temperature transformations. This peak grows in size as one goes to higher zirconium concentrations until near the eutectic (approximately 63 at % Zr), where three peaks become discernible. Increasing the zirconium concentration still further causes the middle peak to grow and go toward lower temperatures while the third peak gradually disappears.

5. Multiple DSC peaks occur at compositions which extend to approximately 3.5 at % Zr on either side of the eutectic composition at 63.5 at % Zr.

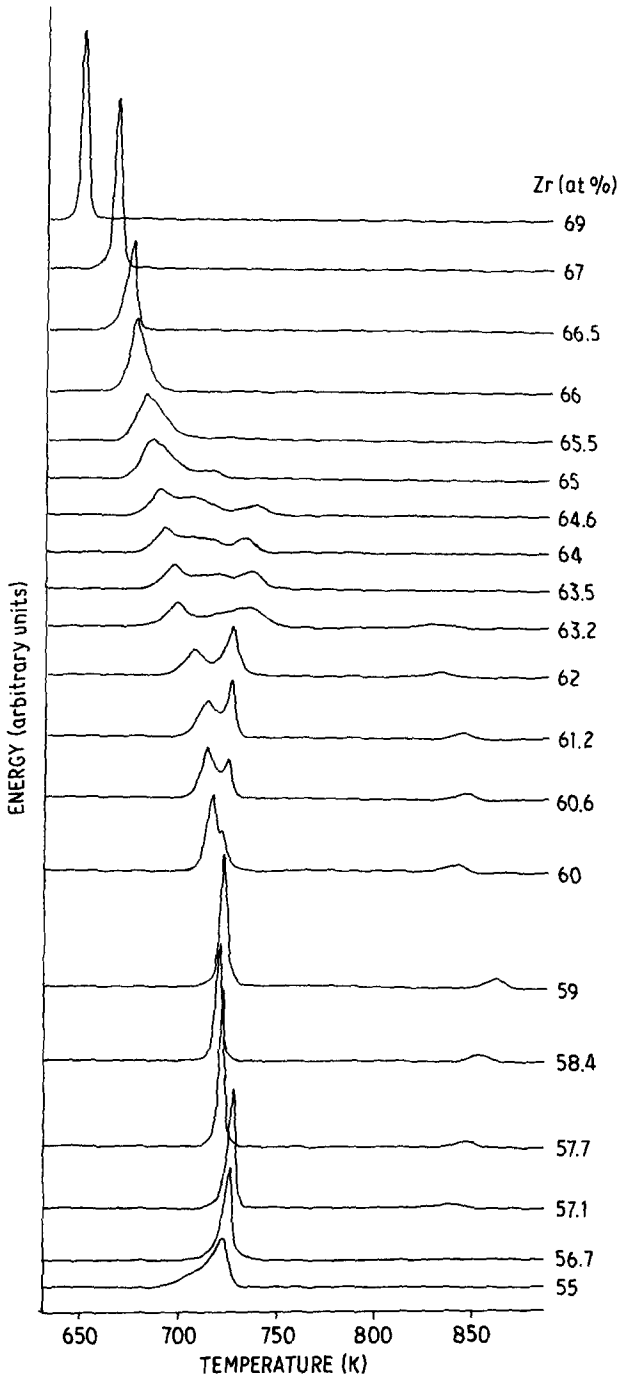

Figure 1 DSC traces produced by the crystallization of Zr–Ni metallic glasses at a heating rate of 20 K min^{-1}.

Calorimetry traces similar to those in Fig. 1 were obtained at 5, 10, 20, 40 and 80 K min^{-1} heating rates for 26 compositions between 55 and 70 at % Zr. From these traces, temperatures T_x, T_{p_1}, T_{p_2}, T_{p_3} and T_{HT} (temperature of the high-temperature peak) were measured. These temperatures are shown as a function of atomic percent zirconium at a heating rate of 20 K min^{-1} in Fig. 2. Where more than one splat was tested, only average values are reported. All the temperature measurements were reproducible to $\pm 2°$. The high-temperatures between 57 and 63.5 at % Zr occurs at temperatures between 825 and 860 K depending on composition, with the maximum temperature occurring at 59 at % Zr.

From the shift in the peak temperature as a function of heating rate, ΔE for each peak was calculated as described earlier. The ΔE values thus obtained are

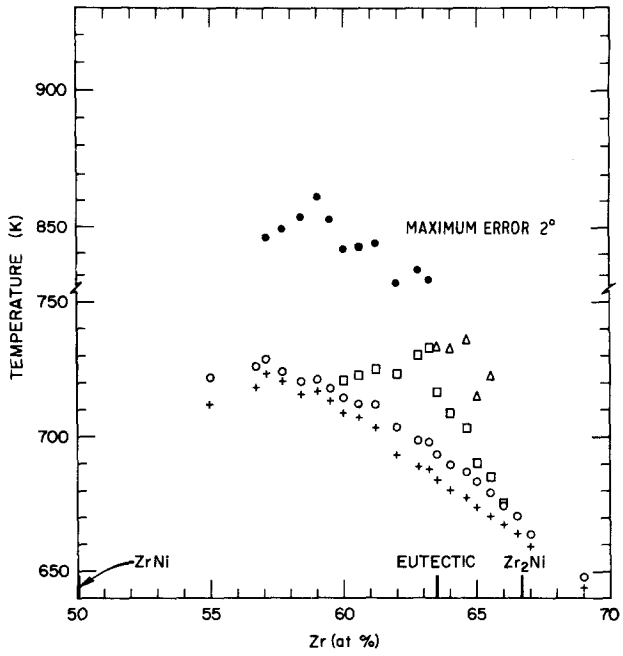

Figure 2 Transformation temperatures as a function of composition for the crystallization of Zr–Ni metallic glasses. The temperatures were taken from DSC traces in which the heating rate used was 20 K min^{-1}. +, Onset of crystallization; ○, 1st DSC peak; □, 2nd DSC peak; △, 3rd DSC peak; ●, high-temperature peak.

shown as a function of composition in Fig. 3. For some compositions there are as many as three data points for each peak (taken from three different splats), indicating reproducibility. The open symbols represent the low-temperature DSC peaks and the darkened symbols the high-temperature peak. The curves are guides to the trends in ΔE and do not represent a mathematical fit to the data. Also, a particular symbol may not always represent the same process, but represents instead the order of appearance on the DSC trace.

The activation energy of the first peak (ΔE_1) exhibits an unusual dependence on composition, indicating changes in the nature of the process occurring. Below approximately 56.7 at % Zr, its value is about 3.2 eV/atom; between 56.7 and 60 its value exhibits a plateau at about 3.8 eV/atom; there is a broad peak reaching to about 4.65 eV/atom between 61.2 and 65 at % Zr; from 66.5 to 71 at % Zr its value is constant at 2.65 eV/atom. Comparison of these composition ranges with the appearance of additional DSC peaks in Fig. 1 suggests a correlation between the appearance of extra DSC peaks and the nature of the first crystallization process. As will be discussed later, it is believed that the nature of the first transformation to occur depends on composition, and that this is reflected in the changes in ΔE_1, as shown in this figure.

The activation energy of the high-temperature peak (ΔE_{HT}) is about 3.5 eV/atom for the 57.1 at % Zr alloy, where it is first discernible. With increasing zirconium content, ΔE_{HT} decreases significantly before it disappears at the eutectic composition, where its value is 2.3 eV/atom.

The second DSC peak, which first appears as a shoulder on the high temperature side of the large transformation peak of $Zr_{60}Ni_{40}$, has a ΔE_2 of 3 eV/atom and remains at about this value as one adds zirconium until the eutectic is reached. However, the alloy at 62.8 at % Zr exhibited a slightly higher ΔE_2 which could not be explained. At the eutectic ΔE_2 decreased drastically to about 2 eV/atom, exhibiting a decrease of 33% within a composition change of only 0.5 at % Zr. From the eutectic composition to near the Zr_2Ni equilibrium compound, ΔE_2 increased linearly to about 2.7 eV/atom.

The activation energy of the third DSC peak (ΔE_3) remains at about 2.6 eV/atom for the composition range where it occurs (63.5 to 65.5 at % Zr).

The enthalpy changes associated with crystallization (ΔH_c) and the high-temperature peak (ΔH_{HT}) were determined from the appropriate areas under the DSC traces and are shown in Figs 4 and 5. The curves are an aid to the eye only. Although difficulty in determining DSC baseline positions unambiguously resulted in an undesirable level of scatter, the data are sufficiently precise for certain salient features of the compositional dependence to be discerned. For example, there are small maxima in ΔH_c at compositions of 67 at % Zr (near the composition of the

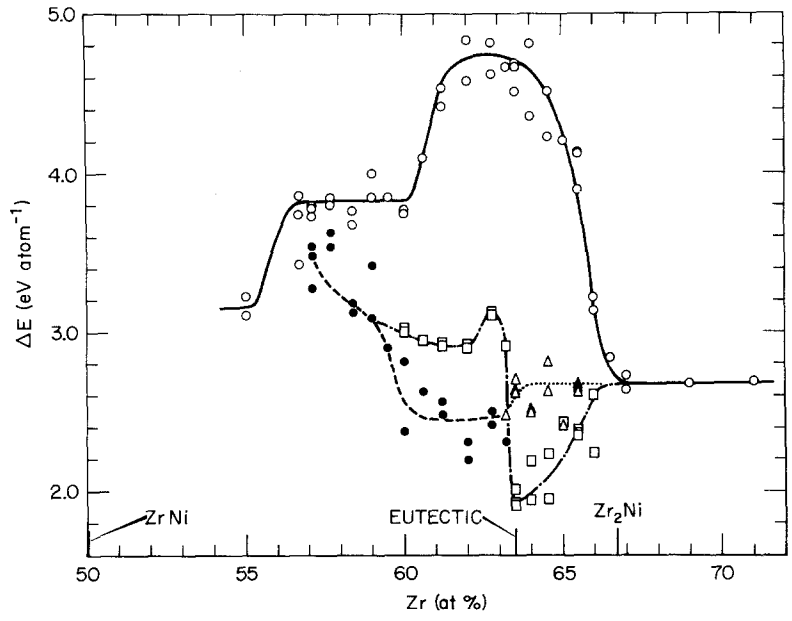

Figure 3 The activation energy (ΔE) as a function of composition for the DSC peaks produced during crystallization of Zr–Ni metallic glasses. ○, ΔE_1; □, ΔE_2; △, ΔE_3; ●, ΔE_{HT}.

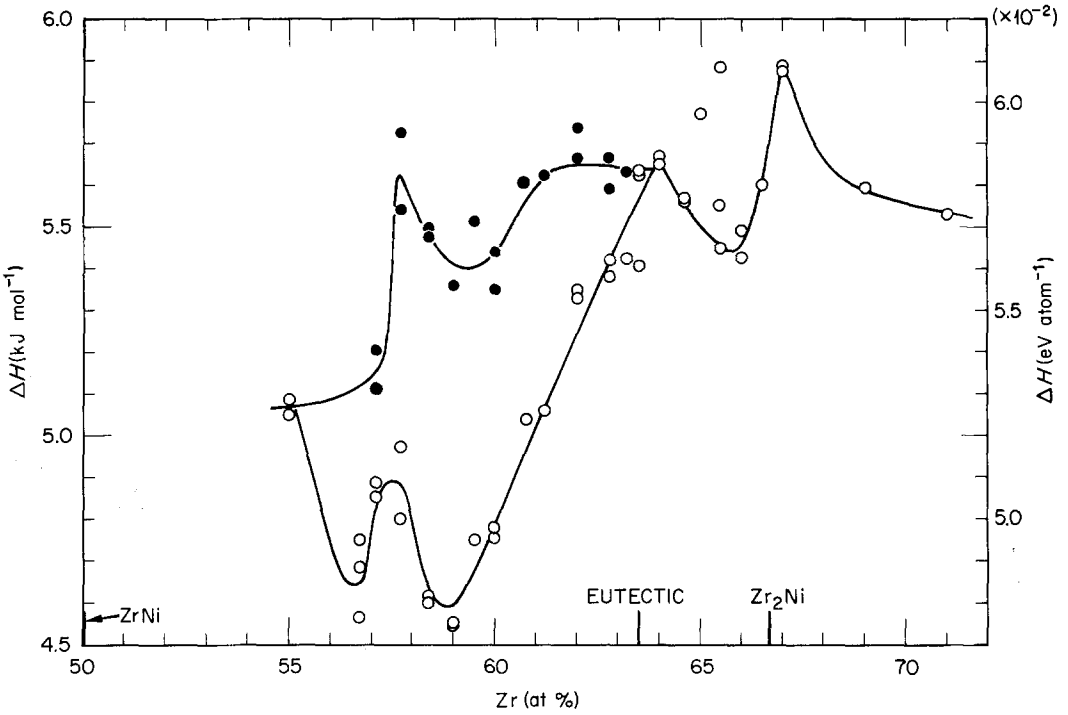

Figure 4 The enthalpy change on heating in the DSC (ΔH) as a function of composition for Zr–Ni metallic glasses. ○, ΔH_c; ●, $\Delta H_t = \Delta H_c + \Delta H_{HT}$.

Zr_2Ni equilibrium phase) and at approximately 57 at % Zr (Fig. 4). A maximum in the total enthalpy change ΔH_t ($\Delta H_t = \Delta H_c + \Delta H_{HT}$) is seen at 57.7 at % Zr. A high plateau in ΔH_t exists between 60.6 and 64 at % Zr. In the composition range where the high-temperature peak is observed, there is a minimum near 59 at % Zr in the ΔH_c value.

Fig. 5 indicates that the high-temperature transformation is first seen at 57.1 at % Zr, and that the compositional dependence of ΔH_{HT} exhibits an asymmetric peak with a maximum value at 58.4 at % Zr.

3.2. Phase identification by X-ray diffraction

The thermal study by DSC indicates that the crystallization process for Zr–Ni metallic glasses in the composition range 55 to 70 at % Zr is very complicated. Assuming that each DSC peak represents a separate transformation, the total crystallization process for a particular composition involves as many as four different transformations. To identify the transformation represented by each DSC peak, several alloy compositions were selected for further study. Pieces of the samples were heated at 80 K min^{-1} in the DSC to particular points on the DSC curve, cooled at 320 K min^{-1} to room temperature, and then studied by XRD. Composite figures similar to Figs. 6 and 7, showing the DSC trace and XRD patterns obtained, were then constructed for each alloy [20]. The XRD patterns were compared with the characteristic patterns of the ZrNi and Zr_2Ni equilibrium phases [21, 22] and with our pattern for the metastable phase noted above [18, 19]. A summary of the transformation products observed as a function of temperature for the selected alloys is given in Table I. From a study of this table and the DSC traces presented in Fig. 1, conclusions can be drawn about the nature of the crystallization process at each composition.

The one DSC peak of $Zr_{55}Ni_{45}$ actually represents two processes occurring at almost the same time. As

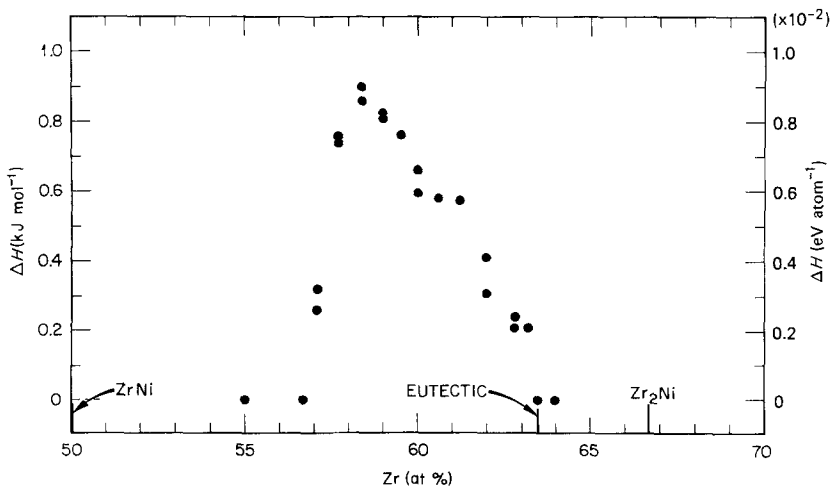

Figure 5 The enthalpy change of the high-temperature peak as a function of composition. The high-temperature peak occurred only at compositions between 57 and 63.5 at % Zr.

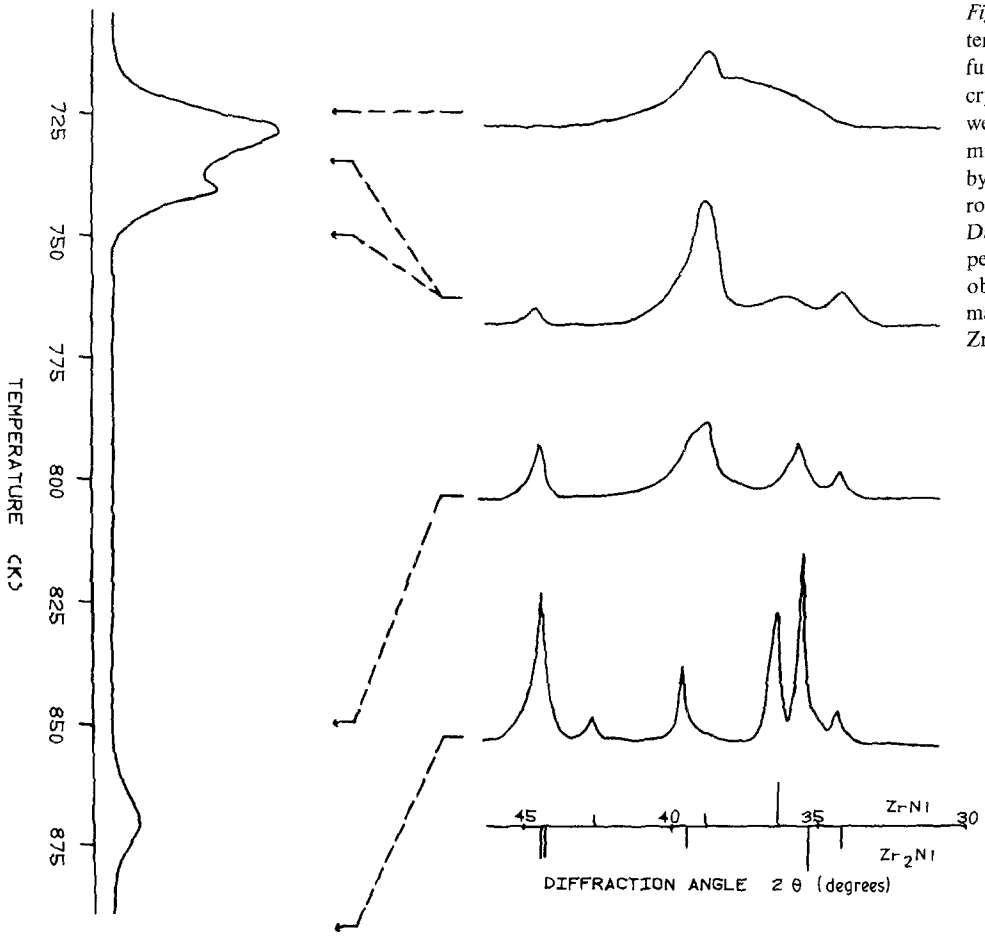

Figure 6 X-ray diffraction patterns obtained for $Zr_{60}Ni_{40}$ as a function of the progression of the crystallization process. Samples were heated in the DSC at 80 K min^{-1} to temperatures indicated by the arrows, then cooled to room temperature at 320 K min^{-1}. Dashed lines connect those temperatures to the X-ray patterns obtained. A scale showing the major X-ray lines for ZrNi and Zr_2Ni is also shown.

seen in Fig. 1, the peak is asymmetrical on the low temperature side, indicating the presence of another peak underneath the main one. The XRD pattern taken after heating to the top of the DSC peak and one of an isothermal anneal at 773 K show lines for both equilibrium phases, ZrNi and Zr_2Ni. However, we were not able to tell which phase appeared first. We assume, since the composition of this alloy is closer to ZrNi than Zr_2Ni, that ZrNi formed first on heating.

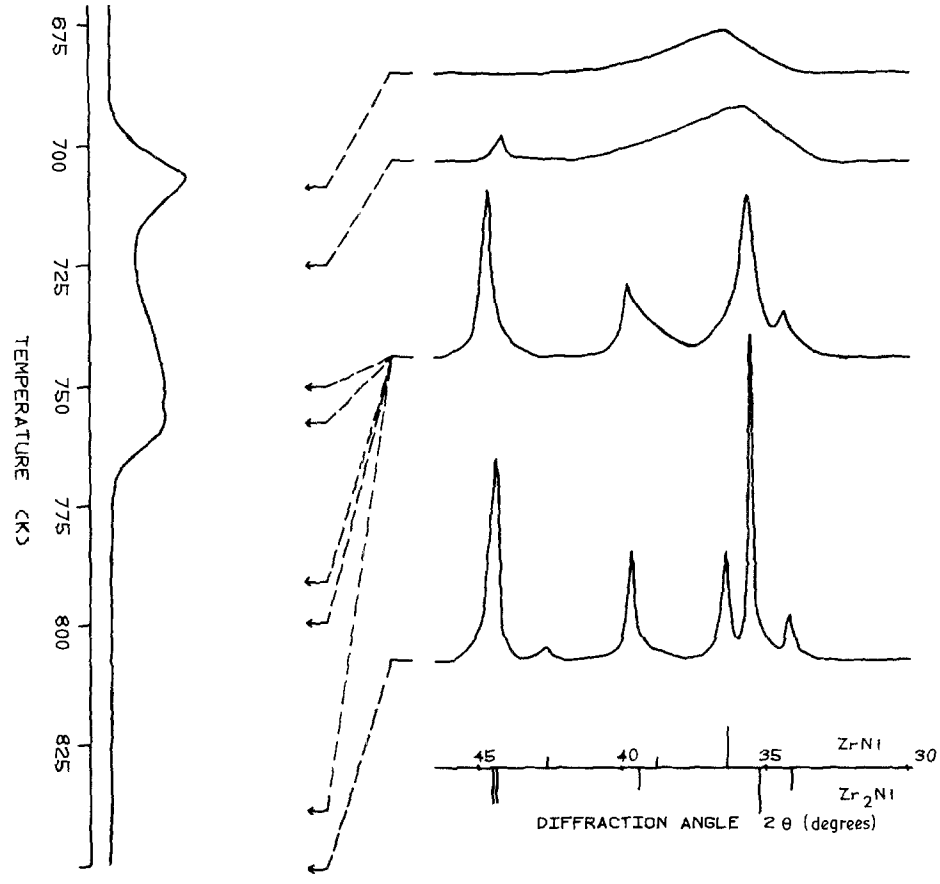

Figure 7 X-ray diffraction patterns obtained for $Zr_{63.5}Ni_{36.5}$ as a function of the progression of the crystallization process. Samples were heated in the DSC at 80 K min^{-1} to temperatures indicated by the arrows, then cooled to room temperature at 320 K min^{-1}. Dashed lines connect those temperatures to the X-ray patterns obtained. A scale showing the major X-ray lines for ZrNi and Zr_2Ni is also shown.

TABLE I Transformation products of Zr–Ni metallic glasses as a function of isochronal DSC annealing at 80 K min^{-1}

Alloy composition (at % Zr)	Temperature at 80 K min^{-1} (K)	Equivalent temperature at 20 K min^{-1} (see Fig. 1)	Phases observed by XRD
55	740	722	Amorphous + ZrNi + Zr_2Ni
	750–785	732–767	ZrNi + Zr_2Ni
57.7	740–760	725–745	Metastable
	860–925	845–910	ZrNi + Zr_2Ni
60	725	710	Amorphous + metastable
	735–750	720–735	Metastable
	850	820	Metastable + Zr_2Ni
	910	880	Zr_2Ni + ZrNi
62	720	705	Amorphous
	735	715	Amorphous + metastable
	750	730	Metastable + Zr_2Ni
	840	810	Metastable + Zr_2Ni
	900	870	Zr_2Ni + ZrNi
63.5	710	695	Amorphous
	725	700	Amorphous + Zr_2Ni
	750–840	715–840	$ZrNi_2Ni$
	860	860	Zr_2Ni + ZrNi
65.5	695	680	Amorphous + Zr_2Ni
	705–765	685–725	Zr_2Ni
	850	825	Zr_2Ni + ZrNi
67	685–780	665–780	Zr_2Ni

The DSC trace for $Zr_{57.7}Ni_{42.3}$ showed a single sharp exotherm at approximately 740 K followed by a small high-temperature peak above 850 K. The XRD pattern taken after annealing to the top of the DSC peak at 740 K showed a strong X-ray line at approximately 38.9° 2θ and a few weaker lines. This same XRD pattern persisted as other pieces of the same splat were annealed to higher temperatures. The X-ray lines could not be indexed to either of the two equilibrium phases (see Table II), and only after annealing into or above the high-temperature peak (860 K or above) were X-ray lines of Zr_2Ni and ZrNi seen. The results indicate that, in the composition range where the high-temperature peak occurs, a metastable phase forms first from the amorphous structure on heating. The high-temperature peak represents the transformation of this metastable phase to equilibrium phases. This metastable phase has been discussed previously by Easton *et al.* [18] and McKamey *et al.* [19], and is being further studied with the hope of determining its structure.

TABLE II X-ray diffraction lines for the equilibrium phases ZrNi and Zr_2Ni as compared to lines of a metastable phase near $Zr_{60}Ni_{40}$

ZrNi [21]		Zr_2Ni [22]		Metastable	
deg 2θ	I (relative)	deg 2θ	I (relative)	deg 2θ	I (relative)*
28.49	10				
				28.96	VW
		34.18	10	34.05	M
				35.15	MW
		35.44	100		
36.50	100				
				37.11	W
				38.59	S
38.93	20				
		39.43	10		
		39.43	30		
				41.97	W
42.81	18				
		44.23	60		
44.35	25	44.38	60	44.35	MW
44.94	44				

*S′ = strong; M = medium; MW = medium to weak; W = weak; VW = very weak.

At $Zr_{60}Ni_4$ (Fig. 6) the first crystalline phase to appear is the metastable phase associated with the first DSC peak (730 K). This alloy has a small second DSC peak at approximately 740 K, which the XRD patterns at 740 or 750 K did not identify. However, after heating to 850 K, which is just below the high-temperature peak, the XRD pattern showed a weakening of the strong line of the metastable phase at 38.9° 2θ and a strengthening of the strong Zr_2Ni lines at 35.5 and 44.4° 2θ. This phenomenon indicates that the second DSC peak at 740 K could represent the formation of Zr_2Ni after the initial formation of the metastable phase. Only after heating to higher temperatures did the Zr_2Ni crystals become large enough to produce detectable peaks in the XRD pattern. Heating into or above the high-temperature DSC peak again produced the equilibrium pattern for this alloy, showing only lines of Zr_2Ni and ZrNi.

At $Zr_{62}Ni_{38}$ the XRD pattern taken after heating to the top of the first DSC peak (720 K) does not indicate that any crystallization has taken place. Instead, the broad diffuse peak typical of an amorphous structure is seen. The first crystalline X-ray peak to appear is the strong line of the metastable phase which occurs after heating into the trough between the two low-temperature DSC peaks (735 K). Just after the second DSC peak, the two strongest X-ray lines of Zr_2Ni (35.5 and 44.4° 2θ) appear. Heating to higher temperatures tends to sharpen the Zr_2Ni lines but does not seem to sharpen the strong line of the metastable phase. After heating to above the high-temperature peak, only Zr_2Ni and ZrNi are seen.

Again in the $Zr_{63.5}Ni_{36.5}$ alloy (Fig. 7), no crystalline X-ray peaks appear until after heating well into the trough following the first DSC peak (725 K). When this first crystalline peak appears, it is not one of the peaks of the metastable phase, but is the strong double peak of Zr_2Ni at 44.4° 2θ. From 750 to 840 K the other Zr_2Ni X-ray lines appear and continue to sharpen. Even though other samples were heated into and above the third crystallization peak, no lines belonging to ZrNi were seen until a temperature of 860 K was reached. However this does not necessarily mean that ZrNi is not present after heating through the crystallization peaks. At this composition, only 18% of the alloy at equilibrium should be ZrNi. Combining this fact with the fact that XRD intensities tend to be low for the ZrNi phase, it is possible that ZrNi is present, but not detected until the crystals have had time to grow. There was no high-temperature DSC peak produced by this alloy, and therefore no metastable phase was formed.

The DSC trace for the $Zr_{65.5}Ni_{34.5}$ alloy shows that the third DSC peak is small (Fig. 1). According to the XRD patterns, Zr_2Ni is the first phase to form, but the X-ray lines of this phase are not detected until the sample has been heated to just above the first DSC peak. Again ZrNi X-ray lines do not appear until the sample has been heated to higher temperatures (850 K), giving the crystals time to grow. Because of this, and the small size of the third DSC peak, we believe the third DSC peak between 63.5 and 65.5 at % Zr represents the formation of the ZrNi phase.

At $Zr_{67}Ni_{33}$ only one DSC peak occurs, which according to the XRD pattern represents the formation of Zr_2Ni from the glass.

4. Discussion

4.1. Comparison of results to previous investigations

The most often reported data on the crystallization of metallic glasses are the crystallization temperatures, activation energies, and enthalpy changes associated with the different DSC transformation peaks. Data of this type for various Zr–Ni compositions between 50 and 70 at % Zr have been published by other researchers [3–8, 11]. The most important differences between our results and those of previous studies are in the number of alloys studied and the use of splat quenched instead of melt-spun samples. We have found significant differences in DSC traces for melt-spun ribbons and arc-hammer quenched splats made from the same casting. We tentatively attribute these differences to differences in oxygen content, perhaps resulting from contact of the melt with the quartz crucible during melt-spinning. Differences in the quench rate or the shape of the cooling curve may also be important. It is our experience that sample-to-sample variations are smaller in splats than in ribbons. Our data for T_x, ΔE, and ΔH therefore show more detail and better indicate the compositions at which crystallization processes change character. Qualitatively, the results of the present study compare well with those of other researchers. In general, T_{p_1} seems to decrease with increasing zirconium content, and a peak is seen in T_{p_2} at approximately 63 to 63.5 at % Zr. However, our temperatures are lower, possibly due to the different quenching method used. Both Dong *et al.* [5] and Buschow *et al.* [6, 11] report T_{p_3} values near the eutectic composition, but do not discuss them in detail. To our knowledge the high-temperature peak between 57 and 63.5 at % Zr, which we found during crystallization of both splat-quenched and melt-spun material, has not previously been reported. Evidence from XRD [18] and from TEM [19] indicates that, in this composition range, the first crystalline phase to form is a metastable phase which transforms to the equilibrium phases on heating through the high-temperature peak.

Our ΔE values are also lower than those reported by other researchers, but we do see a maximum in the ΔE_1 curve around the eutectic, as was seen by Altounian *et al.* [8] and Buschow [11]. As will be discussed later, this maximum in ΔE_1 is associated with the composition range where an exothermic peak occurs on heating in the DSC, but no crystalline lines are produced when the annealed sample is studied by XRD. Our belief is that, compared to glasses near phase compositions, the as-quenched structure of the eutectic composition possesses more disorder. Instead of the nucleation of equilibrium phases, a short range ordering process, as discussed by Wang [23], becomes more thermodynamically and/or kinetically favorable, causing the glass to phase separate into glass structures which are precursors to the Zr_2Ni equilibrium phase and a metastable crystalline phase of composition near Zr_3Ni_2. This concept will be discussed later.

Altounian *et al.* [8] and Henaff *et al.* [13] have presented ΔH data as a function of composition for the Zr–Ni system. Assuming that the enthalpy change on crystallization is almost entirely a change in internal energy between the glass and the crystalline phases, Altounian *et al.* concluded that the ΔH curve could provide a guide to the crystalline phase diagram [8]. They observed maxima at compositions corresponding to the equilibrium phases (ZrNi and Zr_2Ni) and a smaller maximum at $ZrNi_2$ where they believe a previously unreported crystalline phase exists. Our results support the existence of maxima in ΔH at ZrNi and Zr_2Ni. However, we also saw a small peak in ΔH_t between 57 and 58 at % Zr which we associate with the formation of a metastable crystalline phase.

Dong *et al.* [5] and Altounian *et al.* [8] also used XRD to associate DSC peaks with crystallizing phases. Dong *et al.* report that the single DSC peak near 66.7 at % Zr corresponds to the formation of Zr_2Ni. Their attempts at associating DSC peaks with the formation of phases in the 63.5 at % Zr alloy (the eutectic composition) met with the same difficulties as the present study. Three DSC peaks are present and it is difficult to decide which phase belongs to which peak. They saw only equilibrium phases after annealing. At 62 at % Zr, they attribute the two distinct DSC peaks to the crystallization of Zr_2Ni and ZrNi, respectively. Contrary to their results, the XRD results of this study indicate that at 62 at % Zr one has

to anneal well past the first DSC peak before any crystalline X-ray lines are seen. The first line which appears belongs to the metastable phase, and only after the second DSC peak do the lines belonging to Zr_2Ni appear.

Altounian *et al.* [8] used XRD to identify crystallizing phases in the 60, 63.5, and 67 at % Zr alloys. Their results on 67 at % Zr agree with Dong *et al.* and with the results of this study. At 60 and 63.5 at % Zr, XRD patterns taken after heating to just past the first DSC peak showed only the broad diffuse pattern characteristic of the glassy phase. Similar behaviour was also reported in [6, 7, 12]. Altounian *et al.* attribute the second DSC peak in these two alloys to the formation of Zr_2Ni, in agreement with the results of this study.

4.2. Phase separation and chemical short range ordering in Zr–Ni glasses

The question of whether a process which can be called "phase separation" occurs in metallic glasses, either during the liquid-quenching or on subsequent annealing, continues to be debated. The presence of two glass transition temperatures in the Ni–Pd–P [24] and Ti–Be–Zr [25] systems, small-angle X-ray scattering (SAXS) results of the Pd–Au–Si system [26], and transition electron microscopy results of the Fe–B [27] and Ti–Be–Zr [25] systems have been taken as evidence for two glassy phases in these alloys.

In the Zr–Ni system, the reported absence of XRD evidence for crystallization in compositions around the eutectic at 63.5 at % Zr after heating through the first exothermic DSC peak has caused an increased interest in the nature of the transformations at these compositions. Buschow *et al.* [6, 11] and Altounian *et al.* [8] have suggested that the first DSC peak may represent a transition within the amorphous state and comprises mainly short range atomic rearrangements. The strongest evidence for phase separation in the Zr–Ni system has been reported by van Swijgenhoven *et al.* [7]. Because they saw a splitting of the principal SAD ring of an as-quenched 63 at % Zr alloy into two rings, they concluded that $Zr_{63}Ni_{37}$ is phase separated during the rapid quenching process. Their comparison of *d*-values from the SAD rings of amorphous samples with the concentration dependence of the *d*-values determined from XRD led them to infer that the glass sample is phase separated into two glass structures which are precursors of the ZrNi and Zr_2Ni equilibrium crystalline phases. However they note that the glass phase which they believe crystallizes into ZrNi (the first crystals to form) is richer in zirconium than expected.

Recent work by Schultz *et al.* [12] reporting a correlation between chemical short range order (CSRO) and electrical resistivity supports the general conclusions of van Swijgenhoven *et al.* However, Schulz *et al.* believe that the precipitation of very fine grained microcrystalline Zr_3Ni is occurring during the first DSC exotherm.

Likewise, our own previous studies on Zr–Ni glasses have supported the theory of phase separation [1, 2]. From low-temperature specific heat data on a large number of compositions in the range 55 to 75 at % Zr, we observed an unusual composition dependence of electronic properties. Specifically, evidence for two superconducting phases was observed in a splat quenched sample of composition $Zr_{62.9}Ni_{37.1}$. From measurements of the density of states at the Fermi level, superconducting transition temperatures, and ΔH on crystallization, we concluded that the two phases have compositions near $Zr_{60}Ni_{40}(Zr_3Ni_2)$ and $Zr_{66.6}Ni_{33.3}(Zr_2Ni)$. The results of this work were interpreted in terms of an "association model" for liquid alloys, developed by Sommer and Predel, in which associations of atoms with definite stoichiometries exist in equilibrium with unassociated atoms [28, 29].

The present study indicates that this phase separation is most pronounced at the eutectic composition (63.5 at % Zr). At this composition, one has to anneal well past the first DSC peak before crystalline X-ray lines are seen. As one goes away from the eutectic composition in either direction, crystalline X-ray lines are detected earlier, until at 60 and about 65.5 at % Zr, crystalline X-ray lines are detected at the beginning of the first DSC exothermic response. The maximum in ΔE_1 which occurs between 60 and 65.5 at % Zr is believed to indicate the composition range where some degree of phase separation occurs. An explanation for the presence of a maximum in ΔE_1 was discussed by Buschow who studied the relationship of CSRO to composition for various Zr-based metallic glasses [11]. He showed that ΔE for crystallization increased greatly for compositions where CSRO was suspected to occur, especially around the eutectic at $Zr_{63.5}Ni_{36.5}$, in support of our data.

Other researchers have recognized from investigations of the formation, stability, and properties of some amorphous intertransition metal alloys that they may represent a special class of glassy metals whose short-range structure is characterized by a random tetrahedral close-packing of atoms similar to those in their crystalline counterparts [23]. In other words, these amorphous alloys, which include Zr–Ni, may have a "crystal-like" short-range structure that deviates from the dense random packing of hard spheres (DRPHS) model proposed by Bernal [30] and is more like the CSRO of the crystalline phase. Whether this CSRO occurs in the as-quenched alloy or is produced upon heating by a process involving phase separation is not known. Furthermore, the CSRO need not be associated with equilibrium phases. The long range diffusion processes necessary for equilibrium phase formation may not be energetically or kinetically feasible at or near the eutectic composition. Without this long range diffusion, the thermodynamics and kinetics of the system may dictate that crystallization by way of a metastable phase is more probable. The success of this process is enhanced if the CSRO in the glass is similar to that which exists in the metastable phase.

5. Conclusions

From a study of the crystallization of Zr–Ni metallic glasses between 55 and 70 at % Zr by means of thermal analysis and XRD, the following conclusions can be drawn.

1. From 55 to 57 at % Zr, the ZrNi equilibrium

phase forms first from the glassy structure. It probably forms by a primary crystallization process, expelling zirconium into the amorphous matrix. The Zr_2Ni phase begins forming soon after the ZrNi phase.

2. Above approximately 66 at % Zr, Zr_2Ni is the predominant crystalline phase and presumably forms by a polymorphic transformation [4].

3. Between 57 and 66 at % Zr, the crystallization process becomes quite complicated. Eutectic crystallization does not seem to occur. Instead the first phase which forms on the low zirconium side of the eutectic at 63.5 at % Zr is a metastable crystalline phase. The evidence indicates that it has a different morphology than either equilibrium phase [19], the XRD pattern is different, and it transforms to the equilibrium phases upon further heating. The very sharp narrow DSC peak produced by the formation of this metastable phase between 57 and 59 at % Zr indicates that the crystallization of this phase needs little diffusion to proceed and may be occurring by a polymorphic transformation similar to that of Zr_2Ni. Between 60.6 and 63.5 at % Zr, the formation of this phase is preceded by some degree of phase separation and is followed by formation of some Zr_2Ni crystals from the zirconium-enriched matrix. From 63.5 to 66 at % Zr the metastable phase is no longer seen and the first phase to form is Zr_2Ni, followed by ZrNi. Since the eutectic composition does not crystallize eutectically, the Zr_2Ni crystals at this composition probably form by a primary crystallization process [4].

4. A maximum in ΔE_1 between 61 and 65.5 at % Zr indicates that the first stage of crystallization in this composition range is quite different from that of 58 or 67 at % Zr. It is also in this range that, depending on composition, heating into or past the first DSC peak produces XRD patterns showing only the broad diffuse peak characteristic of the amorphous structure. It is believed that this phenomenon is related to the fact that at the eutectic the glass forms more easily on quenching and produces a glass structure with less short range order than the structures produced at 58 or 67 at % Zr. Since TEM micrographs indicate that eutectic crystals do not form at 63.5 at % Zr [4, 20], a process has to occur which involves short range diffusion of atoms and results in a strengthening of the short range order before the formation of crystals can proceed. The results of this study indicate that, between 61 and 65 at % Zr, various amounts of phase separation in the glass structure occur on heating in the DSC. From the results of this study and the low-temperature specific heat data [1, 2], it seems reasonable to assume that it phase separates into glasses of CSRO similar to Zr_3Ni_2 and Zr_2Ni. The maximum in the activation energy is a consequence of that ordering. At 57–59 and 67 at % Zr, the as-quenched glass has the CSRO it needs to proceed with crystallization directly to the metastable phase and Zr_2Ni respectively.

5. The results of this study lend support to recent theories concerning the glass structure proposed by Sommer [28], Predel [29], and Wang [23]. It appears likely that the glass structures of Zr–Ni metallic glasses between 50 and 70 at % Zr are characterized by short-range structures which are similar to or facilitate the formation of those of the crystalline phases to which they crystallize. The degree and type of CSRO in the as-quenched glass may vary according to composition and cooling rate [23]. Our results are consistent with the interpretation that for this system the CSRO of the glass structure around 67 at % Zr is similar to that of Zr_2Ni; at approximately 57 to 59 at % Zr, the CSRO is similar to a metastable crystalline phase of similar composition. The DSC traces for these compositions show single sharp peaks, indicating that the transformation involves a single process with little diffusion necessary. However, near the eutectic where glass-forming tendency is high, extensive ordering during the quench can apparently be avoided. In these compositions (~61 to 65 at % Zr), phase separation upon the first application of heat results in the short-range structures which will eventually transform to the crystalline phases.

Acknowledgements

This research was sponsored by the Division of Materials Sciences, US Department of Energy under contract DE-AC05-84OR21400 with the Martin Marietta Energy Systems, Inc.

The authors would like to acknowledge the cooperation of O. B. Cavin in obtaining the X-ray diffraction results and Gwendolyn Sims for the preparation of the typed manuscript.

References

1. D. M. KROEGER, C. C. KOCH, C. G. MCKAMEY and J. O. SCARBROUGH, *J. Non-Cryst. Solids* **61** (1984) 937.
2. D. M. KROEGER, C. C. KOCH, J. O. SCARBROUGH and C. G. MCKAMEY, *Phys. Rev. B* **29** (1984) 1199.
3. K. H. J. BUSCHOW and N. M. BEEKMANS, *ibid.* **19** (1979) 3843.
4. M. G. SCOTT, G. GREGAN and Y. D. DONG, in Proceedings of the 4th International Conference on Rapidly Quenched Metals, edited by T. Masumoto and K. Suzuki (Japan Institute of Metals, Sendai, 1981) p. 671.
5. Y. D. DONG, G. GREGAN and M. G. SCOTT, *J. Non-Cryst. Solids* **43** (1981) 403.
6. K. H. J. BUSCHOW, B. H. VERBEEK and A. G. DIRKS, *J. Phys. D: Appl. Phys.* **14** (1981) 1087.
7. H. VAN SWIJGENHOVEN, L. M. STALS and K. H. J. BUSCHOW, *Phys. Stat. Solidi A* **72** (1982) 153.
8. Z. ALTOUNIAN, Tu GUO-HUA and J. O. STROM-OLSEN, *J. Appl. Phys.* **54** (1983) 3111.
9. K. H. J. BUSCHOW, I. VINCZE and F. VAN DER WOUDE, *J. Non-Cryst. Solids* **54** (1983) 101.
10. R. FRAHM, *ibid.* **56** (1983) 255.
11. K. H. J. BUSCHOW, *J. Phys. F: Met. Phys.* **14** (1984) 593.
12. R. SCHULZ, V. MATIJASEVIC and W. L. JOHNSON, *Phys. Rev. B* **30** (1984) 6856.
13. M. P. HENAFF, C. COLINET, A. PASTUREL and K. H. J. BUSCHOW, *J. Appl. Phys.* **56** (1984) 307.
14. C. G. MCKAMEY, unpublished data (1984).
15. D. M. KROEGER, W. A. COGHLAN, D. S. EASTON, C. C. KOCH and J. O. SCARBROUGH, *J. Appl. Phys.* **53** (1982) 1445.
16. H. E. KISSINGER, *J. Res. Nat. Bur. Stand.* **57** (1956) 1702.
17. *Idem., Anal. Chem.* **29** (1957) 1702.
18. D. S. EASTON, C. G. MCKAMEY, D. M. KROEGER and O. B. CAVIN, *J. Mater. Sci.* **21** (1986) 1275.
19. C. G. MCKAMEY, D. S. EASTON and D. M. KROEGER, in Proceedings of Materials Research Society

Symposium on Rapidly Solidified Alloys and Their Mechanical and Magnetic Properties, Boston, Massachusetts, December 1984, in press.
20. C. G. MCKAMEY, MSc Thesis, University of Tennessee, 1985.
21. Powder Diffraction File, Sets 19–20, Card No. 19–857 (Joint Committee on Powder Diffraction Standards, Swarthmore, Pennsylvania, 1979).
22. Powder Diffraction File, Sets 11–15, Card No. 12–478, (Joint Committee on Powder Diffraction Standards, Swarthmore, Pennsylvania, 1972).
23. R. WANG, *Nature* **278** (1979) 700.
24. H. S. CHEN, *Mater. Sci. Eng.* **23** (1976) 151.
25. L. E. TANNER and R. RAY, *Scripta Metall.* **14** (1980) 657.
26. C. P. CHOU and D. TURNBULL, *J. Non-Cryst. Solids* **17** (1975) 169
27. J. L. WALTER and S. F. BARTRAM, in Proceedings of the 3rd International Conference on Rapidly Quenched Materials, edited by B. Cantor (The Metals Society, London, 1978) p. 307.
28. F. SOMMER, *Z. Metallkde* **73** (1982) 72.
29. B. PREDEL, *Physica* **103B** (1981) 113.
30. J. D. BERNAL, *Proc. R. Soc.* **A280** (1964) 299.

Received 26 November 1985
and accepted 17 January 1986